Biomedical Physics & Engineering Express

ENDORSED BY IPEM Institute of Physics and Engineering in Medicine

PAPER • OPEN ACCESS

4D flow MRI—Automatic assessment of blood flow in cerebral arteries

To cite this article: Tora Dunås *et al* 2019 *Biomed. Phys. Eng. Express* **5** 015003

Biomedical Physics & Engineering Express

PAPER

4D flow MRI—Automatic assessment of blood flow in cerebral arteries

Tora Dunås[1], Anders Wåhlin[1,2], Laleh Zarrinkoob[3], Jan Malm[3] and Anders Eklund[1,2]

[1] Department of Radiation Sciences, Umeå University, Sweden
[2] Umeå Center for Functional Brain Imaging, Umeå University, Sweden
[3] Department of Pharmacology and Clinical Neuroscience, Umeå University, Sweden

E-mail: tora.dunas@umu.se

Keywords: cerebral arteries, hemodynamics, carotid stenosis, magnetic resonance imaging, circle of willis, cerebrovascular circulation

OPEN ACCESS

RECEIVED
18 September 2018

REVISED
2 October 2018

ACCEPTED FOR PUBLICATION
16 October 2018

PUBLISHED
8 November 2018

Abstract

Objective: With a 10-minute 4D flow MRI scan, the distribution of blood flow to individual arteries throughout the brain can be analyzed. This technique has potential to become a biomarker for treatment decisions, and to predict prognosis after stroke. To efficiently analyze and model the large dataset in clinical practice, automatization is needed. We hypothesized that identification of selected arterial regions using an atlas with a priori probability information on their spatial distribution can provide standardized measurements of blood flow in the main cerebral arteries. *Approach*: A new method for automatic placement of measurement locations in 4D flow MRI was developed based on an existing atlas-based method for arterial labeling, by defining specific regions of interest within the corresponding arterial atlas. The suggested method was evaluated on 38 subjects with carotid artery stenosis, by comparing measurements of blood flow rate at automatically selected locations to reference measurements at manually selected locations. *Main results*: Automatic and reference measurement ranged from 10 to 580 ml min^{-1} and were highly correlated ($r = 0.99$) with a mean flow difference of 0.61 ± 10.7 ml min^{-1} ($p = 0.21$). Out of the 559 arterial segments in the manual reference, 489 were correctly labeled, yielding a sensitivity of 88%, a specificity of 85%, and a labeling accuracy of 87%. *Significance*: This study confirms that atlas-based labeling of 4D flow MRI data is suitable for efficient flow quantification in the major cerebral arteries. The suggested method improves the feasibility of analyzing cerebral 4D flow data, and fills a gap necessary for implementation in clinical use.

List of abbreviations

ICA	Internal carotid artery,
VA	Vertebral artery,
BA	Basilar artery,
PCA	Posterior cerebral artery,
MCA	Middle cerebral artery,
ACA	Anterior cerebral artery,
PCoA	Posterior communicating artery,
CAS	Carotid artery stenosis,
AAIM	Automatic atlas-based artery identification method,
FRQ	Flow rate quantification method

Introduction

4D flow MRI with whole brain coverage makes it possible to assess blood flow in multiple arteries simultaneously (Meckel *et al* 2008, Hope *et al* 2009, Schnell *et al* 2016). Atherosclerosis with stenosis or occlusion of cerebral arteries can affect cerebral blood flow and hemodynamics (Shakur *et al* 2014, Cai *et al* 2016, Wu *et al* 2017). An assessed decreased total blood flow and/or inadequate collateral function of the Circle of Willis has a potential to guide treatment and predict outcome after stroke and risk for recurrent stroke (Henderson *et al* 2000, Amin-Hanjani *et al* 2016).

4D flow MRI is increasingly used for flow assessment (Markl *et al* 2014, Pereira *et al* 2016, Roldán-Alzate *et al* 2016). Today, cerebral 4D flow MRI is processed manually. This requires a skilled operator and is

time-consuming if many arteries are to be investigated. By automatizing this process, flow values can be obtained in a systematic manner, and the operator is free to perform other tasks in the meantime, but this type of automated post-processing tools is missing.

For a method to be considered fully automatic, it is not enough that the delineation of the vessel and separation of vessel lumen from background is automated (van der Geest *et al* 1998, Jiang *et al* 2015), or to automatically find a measurement plane perpendicular to the artery, starting from a manually selected seed point (Wåhlin *et al* 2013, Schrauben *et al* 2015). A fully automatic method should also find the correct placement of the measurements, presenting flow values for all arteries of interest. There has been work presented on fully automatic identification of cerebral arteries (Bogunovic *et al* 2013, Bilgel *et al* 2013), but not aimed specifically on flow quantification, and not adapted for 4D flow MRI.

We have previously developed a cerebral arterial atlas (UBA167), describing the spatial distribution of the main cerebral arteries connected to the Circle of Willis (Dunås *et al* 2016). The atlas consists of a 3D probability maps for each artery, describing the probability that the artery can be found at a particular location in the brain. We have also constructed an arterial identification method (AAIM) utilizing the information from the atlas to enable accurate identification of the main cerebral arteries (Dunås *et al* 2017). We hypothesized that this framework could be expanded to include standardized and automatic assessment of blood flow in these arteries. The challenge for the automatic method is to cope with the inter patient variability in cerebral arterial anatomy and find a measurement position in the identified artery that produce a flow rate estimate that correspond to the one produced when an investigator manually selects the well specified measurement position. Importantly, functionality of such an automatic method should also be robust for deviating flow patterns, e.g. compromised flow caused by a stenosis or occlusion in stroke patients.

Methods

In this study, a new post-processing tool for automatic analysis of 4D flow MRI is presented. This method is based on a previously developed method for arterial labeling where the whole artery is labeled (Dunås *et al* 2016), which in this study is extended to allow for standardized flow measurements.

This new post-processing tool was validated on subjects with carotid artery stenosis (CAS), both in terms of labeling accuracy and flow assessment. For the vessel segmentation and flow quantification we used a previously developed method (Wåhlin *et al* 2013). Automatic measurements were compared to measurements at manually selected locations.

Subjects

Thirty-eight stroke patients with CAS (27 men, 11 women, age 72.5 $\pm$ 5.7 years), admitted to the tertiary stroke center at Umeå university hospital during 2012–2015, were included in this study and investigated with magnetic resonance imaging, including 4D flow MRI.

Inclusion criteria were a transient ischemic attack or stroke, with a corresponding CAS $\geqslant$ 50% on the symptomatic side, and eligible for carotid endarterectomy. Patients with Mini-Mental State Exam <24, modified Rankin scale >2 or ICA occlusion contralateral to the symptomatic side were excluded. Ongoing atrial fibrillation, severe aphasia or other previous neurological disease in the central nervous system were also exclusion criteria. Patients with contraindication for MRI examination were excluded as well. The CAS grading was performed using computed tomography angiography (GE Light Speed VCT 64, Waukesha, WI, USA) data in 31 patients (82%) and carotid artery ultrasound (GE Logiq E9, Linear probe 9L, 9900 Innovation Drive, Wauwatosa, WI, USA or Philips iU22, Linear probe L9-3, 22100, Bothell Everett Highway, Bothell, WA, USA) in 7 patients. The regional ethics review board at Umeå University approved the study and all subject gave informed consent.

MRI

A 3 Tesla scanner (Discovery MR 750; GE Healthcare, Milwaukee, WI, USA) with a 32-channel head coil was used to collect 4D flow MRI (Johnson and Markl 2010). Imaging parameters were: velocity encoding, 110 cm s^{-1}; TR/TE, 6.5/2.7 ms; flip angle, 8°; bandwidth, 166.67 kHz; radial projections, 16 000; acquisition resolution, 300 $\times$ 300 $\times$ 300; imaging volume, 220 $\times$ 220 $\times$ 220 mm^3; reconstruction matrix size, 320 $\times$ 320 $\times$ 320 (zero padded interpolation); and voxel size 0.7 $\times$ 0.7 $\times$ 0.7 mm^3. Velocity maps in x-, y- and z-directions, a T1-weigthed magnitude image and a complex difference angiographic image were reconstructed and used to identify the arteries. No time-resolved data was used in this study, since we were only interested in the time averaged blood flow rate.

Novel approach

The new method is based on a previously developed atlas-based method for artery identification (AAIM). The challenge tackled in this study was to extend this framework to identify specific arterial regions, and to locate seed points for flow quantification corresponding to these regions. Finding such well-defined regions is crucial to obtain reliable flow measurements at standardized locations.

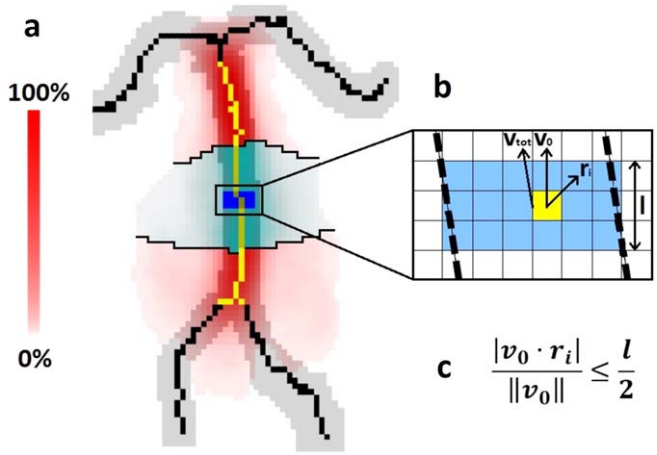

Figure 1. Illustration of labeling and flow calculations in the basilar artery. (a) Labeling: Vessels in grey, centerline in black, probability map for basilar artery in red with the defined atlas region in cyan, candidate voxels in yellow, labeled segment in darker yellow and measurement plane in blue.(b) Zoom in of measurement area shows cross-section calculations, v_0 = velocity direction in the seed voxel, r_i = distance from the seed voxel to voxel i, v_{tot} = average direction of flow for all voxels in the plane. (c) Equation describing inclusion criteria for voxel i.

Flow rate quantification algorithm

The flow rate quantification method (FRQ) used in this study (Wåhlin *et al* 2013) was based on selection of a seed point within the vessel. The velocity vector in the selected seed point was used to determine the direction of the vessel, and blood flow was calculated in a volume defined by two cross-sectional planes perpendicular to this vessel direction, three voxels apart, surrounding the seed point. The equation used to determine which voxels to include in the selected volume is shown in figures 1(b) and (c). The vessel lumen was separated from the background by thresholding the complex difference angiographic image at ten percent of the maximum intensity value. Within the selected volume, flow rates (Q) in x-, y- and z-direction were calculated from the corresponding velocity images, by integrating across the volume and dividing the value by the distance between the two planes.

The flow rate through the arterial volume was calculated as the projection of the total flow on the directional vector of the seed voxel, $|Q| = \cos\theta\sqrt{Q_x{}^2 + Q_y{}^2 + Q_z{}^2}$, where θ is the angle between the flow direction in the seed voxel and the average flow direction within the plane. This approach compensates for misalignment between the initial approximation of the vessel direction and an approximation based on the average flow direction in the vessel.

Manual reference measurements

Two independent raters viewed axial images of the angiographic volume to manually place the seed points for the measurements. The FRQ described above was used to calculate blood flow. In general, the mean flow rate across raters was used as the reference value, although in cases where the difference between the measurements from the two rates in an artery was over 20%, a consensus measurement was made. Because the flow rate in the posterior communicating artery (PCoA) can be very low, it was not feasible to apply the 20% limit to determine if measurements were correct. Therefore, for PCoA, the mean flow rate across raters was used for all cases.

Automatic measurements

Basic principle

The underlying principle of the AAIM was to label voxels within a vascular skeleton according to atlas probabilities. The vascular skeleton of a subject consisted of centerline branches, connected by junction points, where each branch corresponded to a vascular segment and had a unique identification number. To construct this skeleton, the complex difference angiographic image was thresholded to create a binary image, which was then gradually thinned and pruned (Palàgyi and Kuba 1998, Chen and Molloi 2003).

The atlas used for labeling was the UBA167 (Dunås *et al* 2017), which consists of probability maps describing the spatial probability of sixteen large cerebral arteries in Montreal Neurological Institute (MNI) space (Evans *et al* 2012). The labeling took place in the native space of the subject, therefore, using the subjects T1 weighted magnitude image, SPM8's DARTEL (Ashburner 2007) was used to transform the atlas from MNI-space into native space (Dunås *et al* 2016).

Defining measurement sites

To position the seed points in a standardized way, we defined artery specific measurement sites with corresponding regions in the UBA167. Thirteen of the sixteen probability maps in the UBA167 (all except distal ACA and distal MCA) were used in this

implementation, and in ICA and PCA, two regions were defined in the same probability map. These atlas regions where formed as planes with 9 mm thickness and an orientation perpendicular to the arterial segment in question.

The following positions were used for measurements:

- Internal carotid artery (ICA): Vertical petrous segment (C2)
- Internal carotid artery (ICA): Vertical cavernous segment (C4)
- Basilar artery (BA): Middle of artery, between the anterior and superior inferior cerebellar artery
- Vertebral arteries (VA): Vertical intracranial segment (V4)
- Middle cerebral artery (MCA): Proximal main branch (M1)
- Anterior cerebral artery (ACA): Before ACoA aperture (A1)
- Posterior communicating artery (PCoA): Middle of artery
- Posterior cerebral artery (PCA): Just before PCoA aperture (P1)
- Posterior cerebral artery (PCA): Just after PCoA aperture (P2)

All arteries except BA are measured bilaterally, giving a total of 17 defined atlas regions.

Selection of seed voxel

An illustration of the arterial labeling and selection of the seed voxel is presented in figure 1. As for the manual measurements, the FRQ was used for flow calculations. Branch voxels were first labeled according to the probabilities in UBA167, assigning each voxel to the artery with the highest probability. The labeling was then refined by removing voxels that did not fall within the defined atlas regions. Since this transform smoothens the edges of the atlas regions, probability values under 0.3% (half of the lowest value found in the original atlas) were removed before labeling, for both the full UBA167 and for the defined regions. For each region, the longest continuous segment of labeled voxels was identified. Segments shorter than eight voxels (~5 mm) were considered unreliable and were therefore discarded. The midpoint of each identified segment was used as the seed point for the FRQ.

Evaluation

The output from the automatic method, in addition to the flow values, was a 3D image of the vascular system with color-coded regions corresponding to the labeled segments, an example of this labeling is shown in figure 2. These images were visually inspected and each labeled segment was classified as correct or incorrect, based on if the labeled segment corresponded to the correct arterial branch, and accuracy of the labeling method was calculated for each of the nine specified positions. Note that the aim of the labeling process was not to find the whole artery, but to identify a specific segment, selected for accurate flow measurements. Flow values from the automatic method were compared to the manual reference measurements in terms of flow difference.

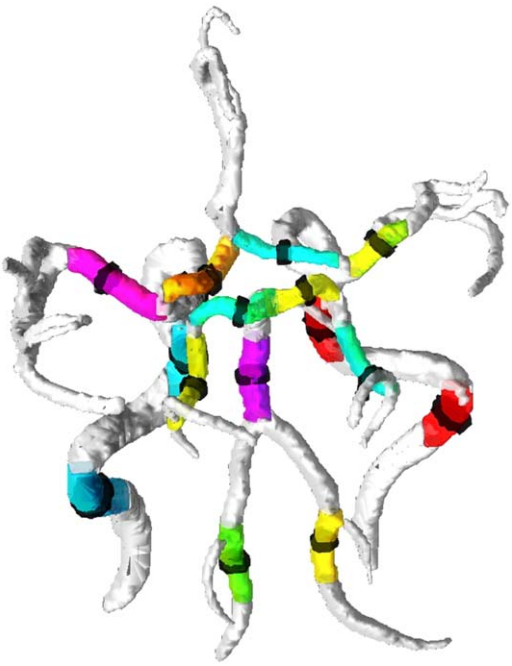

Figure 2. Example of an output image for visual inspection. Gray regions show the regions segmented with arterial blood flow and each colored region corresponds to a labeled segment with black planes indicating the selected seed-points.

Statistical analysis

All data processing and analyses were done in Matlab (Mathworks, Natick, MA, USA). Correlation between automatic and reference measurements was calculated, as well as mean and standard deviation of the difference. Differences between flow rates were tested with paired t-test, significance level was set to $p < 0.05$.

Agreement between the two raters, and between manual and automatic measurements, was evaluated using intraclass correlations (ICC). In both cases, two-way absolute agreement analysis was selected. Since the mean value from the two raters was used as the reference, the multiple measurement option (ICC(2,k)) was used for that analysis, while single measurement (ICC(2,1)) was used when comparing automatic to reference measurements.

Table 1. Results from labeling specified for each artery.

Artery	Total number of arteries	Correctly identified existing (TP)	Correctly identified non-existing (TN)	Mislabeled non-existing (FP)	Mislabeled existing (FN)	Not identified (FN)	Accuracy [%]
ICA C2	73	72	2	1	1	—	97
ICA C4	71	71	5	—	—	—	100
BA	38	38	—	—	—	—	100
VA	66	55	9	1	7	4	84
MCA	76	67	—	—	6	3	88
ACA	69	62	7	—	—	7	92
PCA P1	66	40	9	1	5	21	65
PCA P2	75	71	1	—	3	1	95
PCoA	25	13	41	10	2	10	71
Total	559	489	74	13	24	46	87

True positive (TP), false positive (FP), true negative (TN), and false negative (FN) rates and corresponding accuracy.
ICA - Internal carotid artery, VA - Vertebral artery, BA - Basilar artery, PCA - Posterior cerebral artery, MCA - Middle cerebral artery, ACA - Anterior cerebral artery, PCoA - Posterior communicating artery.

Table 2. Average blood flow in each artery for automatic and reference measurements.

	Flow rate (standard deviation) [ml min^{-1}]			
Artery	Reference	Automatic	Difference	Number of arteries
ICA C2	203.9 (95.8)	204.2 (96.4)	−0.22 (14.3)	72
ICA C4	211.3 (100.7)	213.9 (107.4)	−2.57 (14.7)	71
BA	156.3 (57.9)	157.6 (60.4)	−1.32 (8.2)	38
VA	112.6 (73.5)	116.1 (74.8)	−3.52 (13.3)	55
MCA	129.9 (35.7)	128.8 (37.4)	1.15 (9.4)	67
ACA	97.0 (63.1)	98.6 (64.8)	−1.61 (4.6)*	62
PCA P1	70.1 (28.2)	69.3 (28.6)	0.81 (5.3)	40
PCA P2	58.7 (21.9)	56.7 (22.5)	1.98 (6.6)*	71
PCoA	51.0 (21.5)	51.4 (21.8)	−0.40 (6.9)	13
tCBF	551.1 (101.1)	557.0 (111.3)	−6.12 (22.9)	38

Values are calculated from the correctly identified arteries, total cerebral blood flow (tCBF) is calculated from BA and C4, note that arteries with zero flow have not been included in the flow rate calculations for individual arteries, but are included when calculating tCBF, $^{*}p < 0.05$.
ICA - Internal carotid artery, VA - Vertebral artery, BA - Basilar artery, PCA - Posterior cerebral artery, MCA - Middle cerebral artery, ACA - Anterior cerebral artery, PCoA - Posterior communicating artery.

Results

Manual reference measurements were obtained for 559 arterial segments, whereof 489 were correctly identified by the automatic method. For the 87 arteries were no reference measurements where obtained, 74 were correctly identified as non-existing, yielding a sensitivity of 88%, a specificity of 85%, and an accuracy of 87% when looking at all arterial segments together. Labeling results for each arterial segment are presented in table 1, where the accuracy of 100% in BA and C4 should be specifically noted. The average length of the identified segments was 16.4 ± 3.6 voxels (11.3 mm).

Results from flow quantification are presented in table 2. On average, the flow rate obtained with the automatic measurement was 0.61 ml min^{-1} higher than the manual reference, but this difference was not significant ($p = 0.21$). The standard deviation of the difference compared to the manual reference measurements, across all arteries, was 10.7 ml min^{-1}. The measurements were highly correlated ($r = 0.99$), agreement between the two methods are presented in figure 3.

Intraclass correlation for the different arteries were between 0.95 and 0.99 for the two raters, and between 0.95 and 1.00 for the automatic versus reference measurements. Calculated on all arteries together, both tests gave a intraclass correlation of 0.99. For the comparison of the two raters, all arteries had a 95% confidence interval lower bound over 0.90, and for the automatic versus reference measurements, this was true for all arteries but PCoA.

Discussion

In this study, we described and evaluated a new post-processing tool for 4D flow MRI, where blood flow

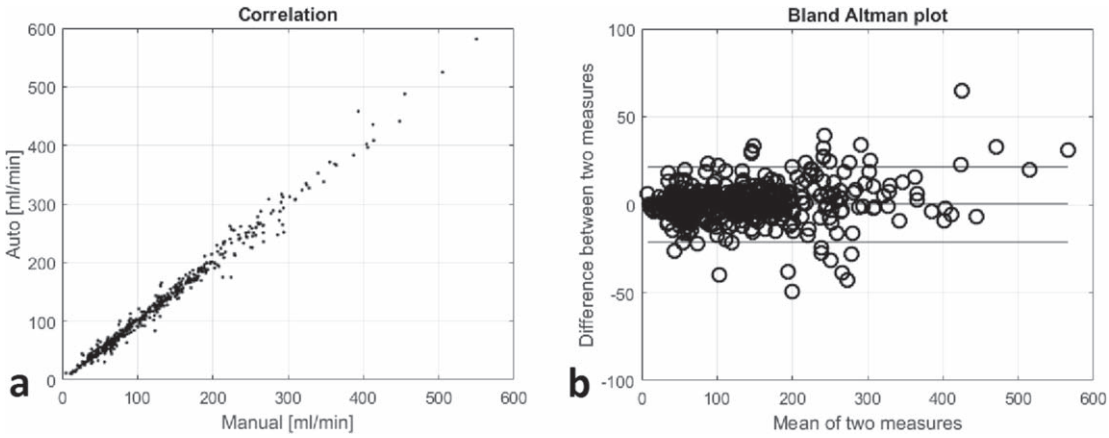

Figure 3. (a) Correlation plot and (b) Bland-Altman plot for the automatic versus reference measurements, with lines representing mean difference and 95% limits of agreements.

rates are automatically calculated in 17 specified arterial regions. Automatic blood flow measurements had an excellent agreement with the manual reference measurements, confirming that atlas-based labeling is suitable for automatic blood flow quantification.

An advantage of 4D flow MRI compared to previous methods such as ultrasound or 2D PCMRI is that data for the entire brain is sampled simultaneously, in a ten-minute MRI sequence. Thus, contrary to 2D PCMRI investigations, it is not necessary for a radiologist to decide in advance which arteries should be examined, or to place and angulate the measurement plane during the MRI acquisition. This work is instead done during the post-processing, and with the method suggested in this study, the time spent on this manual processing could be substantially reduced. The 4D flow MRI collection, together with the post processing described, are so straight forward that it would be possible to implement this new method in clinical routine.

The suggested method had an overall accuracy of 87%, and this accuracy does not seem to be affected by the likely more challenging inter-subject variation in flow rate and morphology in patients with CAS. The automatic seed point selection is supposed to function as an initial placement, with the option to make manual corrections by re-selecting or moving the seed point along the artery if the initial placement was incorrect or unsatisfying.

If flow values are required for all seventeen regions included in this study, manual editing would be needed for 13% of the arteries, but if only the larger cerebral arteries are of interest, this number could be substantially reduced. The new method revealed 100% labeling accuracy in the basilar and distal carotid arteries, making it possible to calculate total cerebral blood flow in all evaluated subjects. For the analysis of the blood supply to the cerebral vascular territories from the Circle of Willis (MCA, ACA, PCA), we have an accuracy between 88 and 95% (table 1). These values are slightly lower than what have been observed for full artery labeling, where these arteries had an accuracy of 96% or higher (Dunås *et al* 2016, Dunås *et al* 2017). This decrease in accuracy is mainly seen in ACA, due to the restricted atlas region, and the MCA, due to the new criteria that only pre-bifurcation segments are considered correctly labeled, which is necessary for correct flow measurements. Even though these values are slightly reduced, they are still considered sufficient for the purpose of this tool. For ICA, BA, VA and PCoA, results are at the same level as previous studies, while P1 have not been previously evaluated.

For MCA, errors occur when the first bifurcation of the M1 segment arises very close to the origin of the artery, resulting in the labeling of a post-bifurcation branch. This error would be easily fixed by manual editing. Lower identification accuracy was obtained for P1, PCoA and VA. If these arteries are required in a specific analysis, for example collateral circulation in the Circle of Willis or cerebellum blood supply, one can expect the need of slightly more editing time.

When looking at flow differences for specific arteries, a significant difference between automatic and manual reference measurements were obtained for ACA and P2, indicating a systematic difference in the placement of the reference measurements compared to the atlas regions. However, the difference was small, and none of the arteries had a systematic difference of more than 4%. The largest difference in flow between automatic and reference measurements was found in the VA. This was likely a manifestation of the highly variable anatomy and the branching of arteries like posterior inferior cerebellar artery, visible in figure 2. Branching arteries that are not included in the atlas does increase the risk of mislabeling, and is the main reason for the low labeling accuracy for VA.

The reported tCBF values are a bit lower than previously reported in healthy elderly (Zarrinkoob *et al* 2015), this is expected in subjects with CAS (Fang *et al* 2016), since the ICA flow is restricted. This is

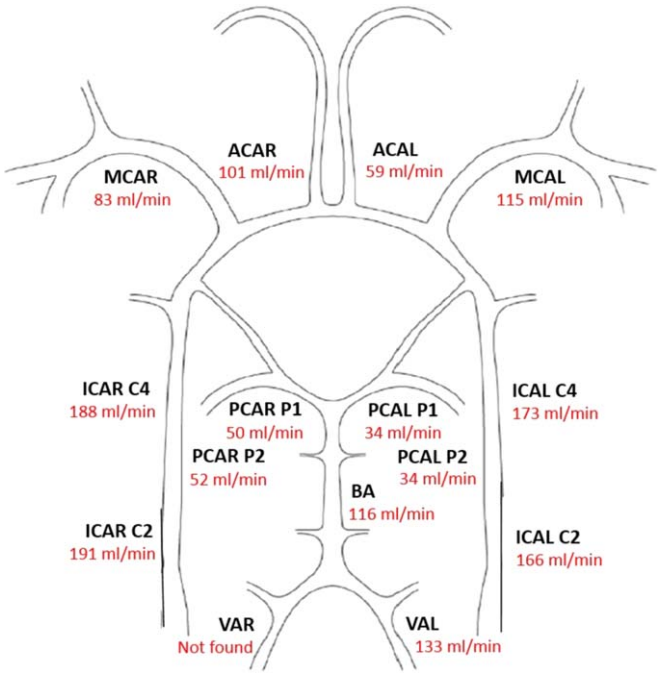

Figure 4. Example of clinical output image ICA - Internal carotid artery, VA - Vertebral artery, BA - Basilar artery, PCA - Posterior cerebral artery, MCA - Middle cerebral artery, ACA - Anterior cerebral artery.

partly, but not completely, compensated by increased blood flow in BA.

The FRQ used in this study is robust and simple, flow values are calculated in a volume with a length of three voxels along the artery. By resampling the neighborhood of the measurement voxel, calculations could be done in a true 2D plane rather than an angled plane through a 3D volume (Schrauben *et al* 2015), which could result in more accurate measurements. It should also be investigated if using a more advanced segmentation than a fixed 10% threshold could give more accurate flow assessment. However, to develop and evaluate the optimal segmentation method, a study designed with an independently measured reference flow, for example with high-resolution 2D PCMRI is needed.

Figure 4 shows a printout report of a 4D flow MRI investigation, produced by the automatic method described in this paper. Blood flow is reported in ml/min for each of the labeled arteries. Although the post-processing of each 4D flow MRI investigation is challenging and consists of a large set of data, calculations are obtained in less than half an hour with the described automated method, not including reconstruction of data, which is necessary for manual measurements as well. Since the process is automated, the only active processing time needed is selecting the cases to analyze, and reviewing the results, the rest of the processing time can be devoted to other tasks.

The post-processing tool described in this paper allows the investigator to quickly get a profile of the distribution of blood flow to the major arteries of the brain. This could for instance be used to study effects of stenosis or carotid artery dissections, or to obtain a risk profile for how well collateral circulation is able to maintain blood flow to the brain's vascular territories (Henderson *et al* 2000, Amin-Hanjani *et al* 2005, Amin-Hanjani *et al* 2016). This may open for a new research area, aiming to use the intracranial blood flow profile for guiding treatment options and to make risk assessments in vascular or neurodegenerative diseases (Rothwell *et al* 2006, Berman *et al* 2015). For example, it could be used to predict how an intracranial stent may change the blood flow profile postoperatively (Alastruey *et al* 2007), or to make preoperative risk assessments of an asymptomatic carotid stenosis (Sheth and Liebeskind 2014, Pereira *et al* 2016).

In conclusion, atlas-based labeling was suitable for automatic quantification of cerebral blood flow in 4D flow MRI. In total, 87% of all arteries were correctly labeled, with 100% accuracy for the large supplying arteries needed to calculate total cerebral blood flow. Agreement between automatic and manual reference measurements was excellent, with no systematic difference and a higher stability than repeated manual measurements. This study demonstrates the feasibility and utility of the atlas-based approach to assess cerebral arterial blood flow. It provides the tool for analyzing cerebral 4D flow MRI data that is needed for efficient *in vivo* study of arterial blood flow in the brain and should have important applications in various neurological diseases.

Acknowledgments

This study was supported by the Swedish Research Council [grant number 2015-05616] and the Swedish

Heart-Lung Foundation [grant numbers 20110383, 20140592].

ORCID iDs

Tora Dunås https://orcid.org/0000-0002-5911-9511
Jan Malm https://orcid.org/0000-0001-6451-1940

References

Alastruey J *et al* 2007 Modelling the circle of Willis to assess the effects of anatomical variations and occlusions on cerebral flows *J. Biomech.* **40** 1794–805
Amin-Hanjani S *et al* 2016 Effect of hemodynamics on stroke risk in symptomatic atherosclerotic vertebrobasilar occlusive disease *JAMA Neurology* **73** 178–85
Amin-Hanjani S *et al* 2005 Use of quantitative magnetic resonance angiography to stratify stroke risk in symptomatic vertebrobasilar disease *Stroke* **36** 1140–5
Ashburner J 2007 A fast diffeomorphic image registration algorithm *NeuroImage* **38** 95–113
Berman S E *et al* 2015 Intracranial arterial four-dimensional flow is associated with metrics of brain health and Alzheimer's disease *Alzheimer's and Dementia: Diagnosis, Assessment and Disease Monitoring* **1** 420–8
Bilgel M *et al* 2013 Automated anatomical labeling of the cerebral arteries using belief propagation *Proc. of SPIE Int Soc Opt Eng* vol 866918, pp 1– 6
Bogunovic H *et al* 2013 Anatomical labeling of the circle of willis using maximum a posteriori probability estimation *IEEE Trans. Med. Imaging* **32** 1587–99
Cai J *et al* 2016 Comparison of extracranial artery stenosis and cerebral blood flow, assessed by quantitative magnetic resonance, using digital subtraction angiography as the reference standard *Medicine* **95** e5370
Chen Z and Molloi S 2003 Automatic 3D vascular tree construction in CT angiography *Comput. Med. Imaging Graph.* **27** 469–79
Dunås T *et al* 2017 A stereotactic probabilistic atlas for the major cerebral arteries *Neuroinformatics* **15** 101–10
Dunås T *et al* 2016 Automatic labeling of cerebral arteries in magnetic resonance angiography *Magn. Reson. Mater. Phys. Biol. Med.* **29** 39–47
Evans A C *et al* 2012 Brain templates and atlases *NeuroImage* **62** 911–22
Fang H *et al* 2016 Compensatory patterns of collateral flow in stroke patients with unilateral and bilateral carotid stenosis *BMC Neurology* **16** 4–9
Henderson R D *et al* 2000 Angiographically defined collateral circulation and risk of stroke in patients with severe carotid artery stenosis *Stroke* **31** 128–33
Hope M D *et al* 2009 Complete intracranial arterial and venous blood flow evaluation with 4D flow MR imaging *American Journal of Neuroradiology* **30** 362–6
Jiang J *et al* 2015 Quantifying errors in flow measurement using phase contrast magnetic resonance imaging: comparison of several boundary detection methods *Magn. Reson. Imaging* **33** 185–93
Johnson K M and Markl M 2010 Improved SNR in phase contrast velocimetry with five-point balanced flow encoding *Magn. Reson. Med.* **63** 349–55
Markl M, Schnell S and Barker A J 2014 4D flow imaging: current status to future clinical applications *Current Cardiology Reports* **16** 481
Meckel S *et al* 2008 *In vivo* visualization and analysis of 3D hemodynamics in cerebral aneurysms with flow-sensitized 4D MR imaging at 3 T *Neuroradiology* **50** 473–84
Palàgyi K and Kuba A 1998 A 3D 6-subiteration thinning algorithm for extracting medial lines *Pattern Recognit. Lett.* **19** 613–27
Pereira V M *et al* 2016 4D Flow MRI in neuroradiology : techniques and applications *Topics in Magnetic Resonance Imaging* **25** 81–7
Roldán-Alzate A *et al* 2016 Emerging applications of abdominal 4D flow MRI *American Journal of Roentgenology* **207** 58–66
Rothwell P M, Buchan A and Johnston S C 2006 Recent advances in management of transient ischaemic attacks and minor ischaemic strokes *Lancet Neurology* **5** 323–31
Schnell S, Wu C and Ansari S A 2016 Four-dimensional MRI flow examinations in cerebral and extracerebral vessels–ready for clinical routine? *Current Opinion in Neurology* **29** 1–10
Schrauben E *et al* 2015 Fast 4D flow MRI intracranial segmentation and quantification in tortuous arteries *Journal of Magnetic Resonance Imaging* **42** 1458–64
Shakur S F *et al* 2014 Effects of extracranial carotid stenosis on intracranial blood flow *Stroke* **45** 3427–9
Sheth S A and Liebeskind D S 2014 Imaging evaluation of collaterals in the brain: physiology and clinical translation *Current Radiology Reports* **2** 29
van der Geest R J *et al* 1998 Automated measurement of volume flow in the ascending aorta using MR velocity maps: evaluation of inter- and intraobserver variability in healthy volunteers *J. Comput. Assist. Tomogr.* **22** 904–11
Wu X C *et al* 2017 *In vivo* assessment of the impact of regional intracranial atherosclerotic lesions on brain arterial 3D hemodynamics *American Journal of Neuroradiology* **38** 515–22
Wåhlin A *et al* 2013 Measuring pulsatile flow in cerebral arteries using 4D phase-contrast MR imaging *American Journal of Neuroradiology* **34** 1740–5
Zarrinkoob L *et al* 2015 Blood flow distribution in cerebral arteries *Journal of Cerebral Blood Flow & Metabolism* **35** 648–54